THE PUBLISHING HOUSE
OF THE ROMANIAN ACADEMY

PROCEEDINGS OF THE ROMANIAN ACADEMY, Series A,
Volume 26, Number 2/2025, pp. 173–182
DOI: 10.59277/PRA-SER.A.26.2.08

ANALYZING FLOW AND THERMAL BEHAVIOR IN LAMINAR MIXED CONVECTION: EFFECTS OF ROTATING CYLINDER LOCATED AT VARIOUS SIDE WALLS

Abdelkader FILALI[1], Farid BERRAHIL[2,3], Hamza SEMMARI[1], Abdellatif M. SADEQ[4]

[1] Ecole Nationale Polytechnique de Constantine, LMSEA Laboratory, BP75, A, Ali Mendjli, 25000 Constantine, Algeria
[2] University of Frères Mentouri-Constantine 1, Faculty of Sciences Technology, Department of Mechanical Engineering, LEAP Laboratory, Constantine, Algeria
[3] University Center Abdelhafid Boussouf, Science and Technology Institute, Mila, Algeria
[4] Independent Researcher, Mechanical Engineering, Doha, Qatar
Corresponding author: Abdelkader FILALI, E-mail: filali.abdelkader@enp-constantine.dz

Abstract. The present study investigates numerically the laminar mixed convection problem in a square enclosure with a mounted rotating cylinder at different sidewalls. The goal is to characterize the geometrical model that performs the best and offers the highest heat transfer rate by relocating the rotating cylinder. The effect of the cylinder angular speeds defined by *Re* number for a wide range of ($100 \leq Re \leq 1200$) and Grashof number of ($7\times10^3 \leq Gr \leq 4.9\times10^4$), and the effect of the cylinder radius R_0, on the heat transfer characteristics are considered. The suggested geometry is a square cavity with a bottom wall that is immobile and heated to a temperature of T_h and with rotating cylinders mounted at different sidewalls and maintained at cold temperature T_c. Remaining walls are considered adiabatic. Results revealed that flow patterns and thermal performance are directly affected by the placement location of both the chosen heated wall and the rotating cylinder. From the four investigated geometrical models, case A (cold cylinder located at the top wall of the cavity + cavity left wall heated), was found to be the best performing geometrical model in the range of the investigated flow and thermal parameters with a maximum value of $Nu_{max} = 9.183$ for $Ri = 0.034$. It was also found that increasing the rotating cylinder radius R_0 leads to an enhanced heat transfer rate.

Keywords: square cavity, rotating cylinder, mixed convection, maximum heat transfer.

Nomenclature

g – gravitational acceleration, m/s^2
Gr – Grashof number
L – Cavity's side length, m
Nu – average Nusselt number
Nu_{max} – maximum average Nusselt number
p – pressure, N·m^{-2}
P – non-dimensional pressure
Pr – Prandtl number
r_o – cylinder radius, m
R_0 – non-dimensional cylinder radius
Ra – Rayleigh number
Re – Reynolds number
Ri – Richardson number
T_c – cold temperature, K
T_h – hot temperature, K
u, v – velocity component, m·s^{-1}
U, V – non-dimensional velocity components
x, y – horizontal and vertical coordinates, m
X, Y – non-dimensional horizontal and vertical coordinates

Greek Symbols

ν – kinematic viscosity, m^2 s^{-1}
α – thermal diffusivity, m^2 s^{-1}
β – thermal expansion coefficient, K^{-1}
θ – dimensionless temperature
ω – angular speed of the rotating cylinder, rad·s^{-1}
Ω – dimensionless angular speed of the rotating cylinder

1. INTRODUCTION

Heat transfer through natural convection in partially heated enclosures has been extensively studied [1]. Enhancing heat transfer often involves modifying the system's configuration. Lid-driven cavities with moving walls and rotating components, such as internal cylinders or arc-shaped rotating walls, improve convection by introducing mixed convection effects [2–6]. The direction of wall or obstacle movement can significantly influence thermal performance, which is crucial for applications like electronic cooling, solar collectors, and building ventilation [7–9].

Geometric modifications also play a key role in optimizing heat transfer. Modifications such as wavy walls [10], artificial roughness [11], internal heaters or fins [12], and fixed obstacles of various shapes circular, elliptical, triangular, square, and rectangular, are commonly used to alter flow structures [13–18]. Rotating obstacles, especially cylinders, are effective in improving heat transfer rates. Given their relevance to practical systems, optimizing geometries with rotating cylinders has become an important research focus. Several studies have explored such designs using numerical methods [19, 20]. For instance, Dos Santos et al. [21] and Lorenzini et al. [22] examined fin-enhanced enclosures, while Hussain and Hussein [23] showed that cylinder position and governing parameters like Reynolds and Richardson numbers significantly affect performance. Park et al. [24] demonstrated that reduced distance heated and cooled surfaces increases the Nusselt number.

Recent investigations, such as those by Razera et al. [25, 26], focused on optimizing fin shapes and positions, confirming that factors like fin geometry and placement impact heat transfer. Muneer [6] found that arc-shaped rotating walls effectively enhance convection. Overall, thermal performance is governed by the balance of natural and forced convection, the orientation of rotating elements, and their interaction with buoyant forces.

To the best of the authors' knowledge, the uniqueness of the present study lies in its focus on a mixed convection flow in lid-driven cavities featuring a rotating cylinder mounted on the sidewalls of the enclosure. This specific configuration has not been explored in previous research, making it a novel contribution to the field. While prior studies have examined various aspects of mixed convection in cavities and the influence of rotating cylinders, the combination of these two elements in the context of sidewall-mounted cylinders within a lid-driven cavity remains unaddressed in the literature, thus highlighting the originality of this investigation. The chosen configuration has various practical applications: For lower Prandtl numbers ($Pr \sim 1$), such as air or gases, it represents scenarios like rotating electronic components positioned along enclosure edges, heat wheels, or engine blocks with rotating cylinders. For higher Prandtl numbers ($Pr > 7$), it applies to lubricated rotating cylinders, bearings in water or oil baths, or coating processes.

2. GEOMETRY AND MESHING STRATEGY

This study aims to identify the best-performing geometrical model for laminar mixed convection in a lid-driven cavity with a clockwise-rotating cold cylinder embedded in one sidewall. As shown in Figure 1, four configurations are tested: (A) cylinder at the top wall, left wall heated; (B) cylinder at the top wall, bottom wall heated; (C) cylinder at the right wall, left wall heated; and (D) cylinder at the bottom wall, left wall heated. All other walls are adiabatic. The cavity is filled with air, assuming constant properties ($Pr = 0.71$), with density variation modeled using the Boussinesq approximation. The objective is to determine which configuration yields the highest heat transfer across a range of Reynolds numbers ($100 \le Re \le 1200$) and Grashof numbers ($7\times10^3 \le Gr \le 4.9\times10^4$). The combined influence of Re and Gr is captured by the Richardson number $0.0048 \le Ri \le 4.9$, covering various convection regimes.

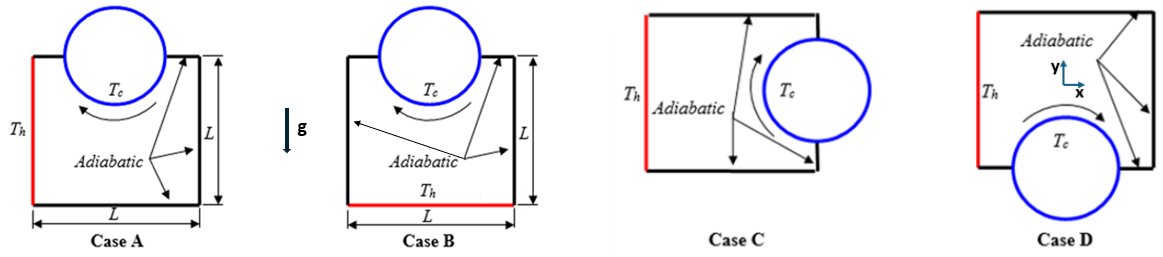

Fig. 1 – Physical domain of the considered problem.

Several grid sizes were evaluated, including configurations of 100×140, 140×160, 160×180, and 180×200. The comparison of the computed average Nusselt number, illustrated in Fig. 2, indicates that the mesh of 160×180 cells provides the best compromise, providing accurate Nusselt number results with efficient computation.

Further analysis on the effect of the rotating cylinder radius on the heat transfer is considered. Three dimensionless cylinder radius of R_0 = 0.8, 0.5 and 0.2 are considered for the case A only.

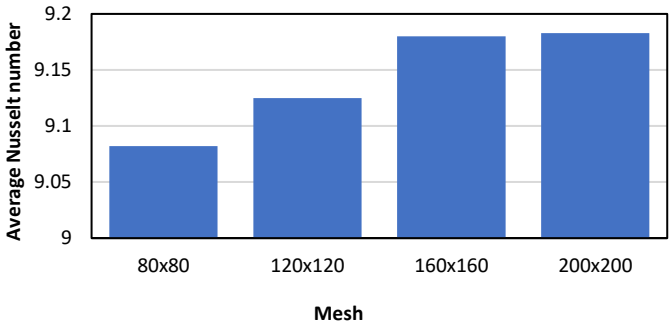

Fig. 2 – Grid sensitivity test for the case A, Re = 1200 and Gr = 4.9x10^4.

3. MATHEMATICAL FORMULATION

For a steady-state laminar convection problem in a 2D laminar air flow, the governing equations of mass, momentum, and energy conservation are defined using the following non-dimensional forms:

$$\frac{\partial U}{\partial X}+\frac{\partial V}{\partial Y}=0 \tag{1}$$

$$\frac{\partial U}{\partial X}+V\frac{\partial U}{\partial Y}=-\frac{\partial P}{\partial X}+\frac{1}{Re}\left(\frac{\partial^2 U}{\partial X^2}+\frac{\partial^2 U}{\partial Y^2}\right) \tag{2}$$

$$U\frac{\partial V}{\partial X}+V\frac{\partial V}{\partial Y}=-\frac{\partial P}{\partial Y}+\frac{1}{Re}\left(\frac{\partial^2 V}{\partial X^2}+\frac{\partial^2 V}{\partial Y^2}\right)+Ri\cdot\theta \tag{3}$$

$$U\frac{\partial \theta}{\partial X}+V\frac{\partial \theta}{\partial Y}=\frac{1}{Re\cdot Pr}\left(\frac{\partial^2 \theta}{\partial X^2}+\frac{\partial^2 \theta}{\partial Y^2}\right) \tag{4}$$

The definition of each used dimensionless quantity is

$$(X,Y)=\frac{(x,y)}{L},\ R_0=\frac{r_0}{L},\ (U,V)=\frac{(u,v)L}{\alpha},\ P=\frac{(p+\rho gy)}{\rho\alpha^2},\ \theta=\frac{T-T_c}{T_h-T_c},$$
$$Re=\frac{\omega r_0 L}{\nu},\ Pr=\frac{\nu}{\alpha},\ \Omega=\frac{\omega L^2}{\alpha},\ Gr=\frac{Ra}{Pr} \tag{5}$$

where Rayleigh number Ra is expressed as:

$$Ra=\frac{g\beta(T_h-T_c)L^3}{\nu\alpha} \tag{6}$$

So, Richardson number Ri is expressed as:

$$Ri=\frac{Gr}{Re^2}=\frac{Ra\cdot Pr}{\Omega^2 R_0^2} \tag{7}$$

The rotating cylinder center lies along one of the cavity walls with the dimensionless coordinates and its dimensionless radius defined as (X_0, Y_0, R_0) = (x_0, y_0, r_0) / L.

The dimensionless magnitude of the velocity at the rotating cylinder surface is defined as:

$$|V|=\sqrt{U^2+V^2}=\Omega R_0 \tag{8}$$

where $U=\Omega\,(Y-Y_0)$ and $V=-\Omega\,(X-X_0)$.

All fluid properties are assumed to be constant, except the fluid density, which is subject to temperature variations and adheres to the Boussinesq approximation; these fluid properties are considered constant [1]. The assumption of constant fluid properties is a valid simplification under moderate temperature gradients. This assumption has been commonly adopted in previous laminar mixed convection studies [2, 5, 6, 15, 17, 26], where the variation in properties was shown to have negligible influence on the overall flow structure and heat transfer characteristics under similar conditions. The average Nusselt number is determined as follows:

$$Nu = \int_0^1 Nu(X)\,\mathrm{d}X \qquad \text{or} \qquad Nu = \int_0^1 Nu(Y)\,\mathrm{d}Y \tag{9}$$

where $Nu\,(X)$ and $Nu\,(Y)$ are the local Nusselt numbers in the horizontal and vertical directions, respectively, defined as:

$$Nu(X) = -\frac{\partial\theta}{\partial Y}\bigg|_{Y=0} \quad \text{or} \quad Nu(Y) = -\frac{\partial\theta}{\partial X}\bigg|_{X=0} \tag{10}$$

4. NUMERICAL METHOD

The governing equations, denoted by Eqs. (1)–(4), are numerically resolved using the finite volume technique in ANSYS Fluent. The well-known SIMPLE algorithm [27] is used to couple the pressure and velocity fields. To guarantee the correctness of the solution, a convergence criterion with a tolerance of 10^{-6} is applied to all variables. To improve the accuracy of the results, the second-order upwind technique is utilized for discretizing the pressure, convection term, and energy equation, thus minimizing numerical diffusion and increasing the overall solution fidelity. The present numerical results were validated with the experimental results of Krane and Jessee [28] for natural convection in a cavity filled with air for $Ra = 10^5$ and $Pr = 0.7$. The air properities are assumed constant except the density which is estimated using the Boussinesq approximation. The cavity's left wall is maintained at hot temperature T_h and the right wall is maintained at a cold temperature T_c. As illustrated in Fig. 3, the comparison of the temperature profile across the cavity width show an excellent agreement between the present results and the experimental results reported by Krane and Jessee [28].

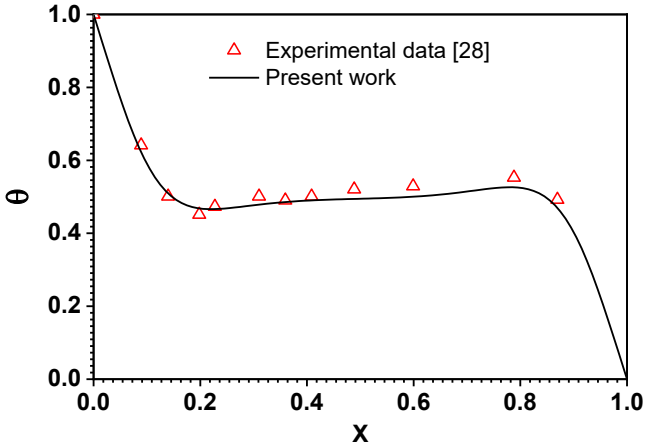

Fig 3 – Temperature profile across the cavity width. Comparison of the present study's results with the experimental data [38] for $Ra = 10^5$ and $Pr = 0.7$.

5. RESULTS AND DISCUSSION

The study investigates how the rotating cylinder's location and size affect heat transfer in a mixed convection system. It analyzes three positions right, top, and bottom and explores how changes in cylinder radius influence thermal performance.

5.1. Flow and thermal behavior

The streamlines and isotherms for the investigated cavity with rotating cylinder for the different cases A, B, C and D are presented in Figs. 4, 5, 6 and 7, respectively. The discussion is organized by considering *Re* and *Gr* numbers as follows:

For case A. As shown in Fig. 4, the cavity's left wall is heated to temperature T_h, and a rotating cylinder is located at the top wall. For $Gr = 7\times10^3$ and Reynolds numbers ranging from 100 to 600, the flow develops three vortices: a dominant top vortex occupying over 85% of the cavity, a medium-sized vortex in the lower-left corner, and a smaller one in the lower-right corner. As Re increases, the medium vortex shrinks, while the smaller vortex alternates in size-shrinking at $Re = 300$ and expanding again at $Re = 600$. At $Re = 1\,200$, intensified flow near the top-left corner suppresses the bottom vortices, leaving two major vortices.

As Gr increases to 4.9×10^4, natural convection dominates, enlarging the bottom vortex. The two main vortices align horizontally, and the top vortex shifts toward the upper-left, exhibiting stronger flow patterns.

In the isotherms, higher Re leads to a thinner hot layer along the left wall due to the cold flow displacing hot fluid. This compresses the thermal boundary layer and enhances heat transfer through stronger interaction between the incoming cold flow and the hot fluid near the heated wall.

For case B. Figure 5 shows the cavity's bottom wall heated to T_h, with a rotating cylinder at the top. For varying Gr number and $Re = 100$ and 300, two main vortices appear: a large one covering about 95% of the cavity and a smaller one in the lower-left corner. At $Re = 600$, a third vortex forms in the lower-right, and the lower-left vortex grows with increasing Re. At $Re = 1200$, two large horizontal vortices dominate, dividing the cavity and minimizing Gr's effect due to strong forced convection.

For isotherms, case B shows better cold fluid transport to the center than case A, but at $Re = 1200$, the top-left vortex hinders cold air movement. Higher Gr increases air temperature, showing stronger buoyancy forces affect thermal and flow behavior.

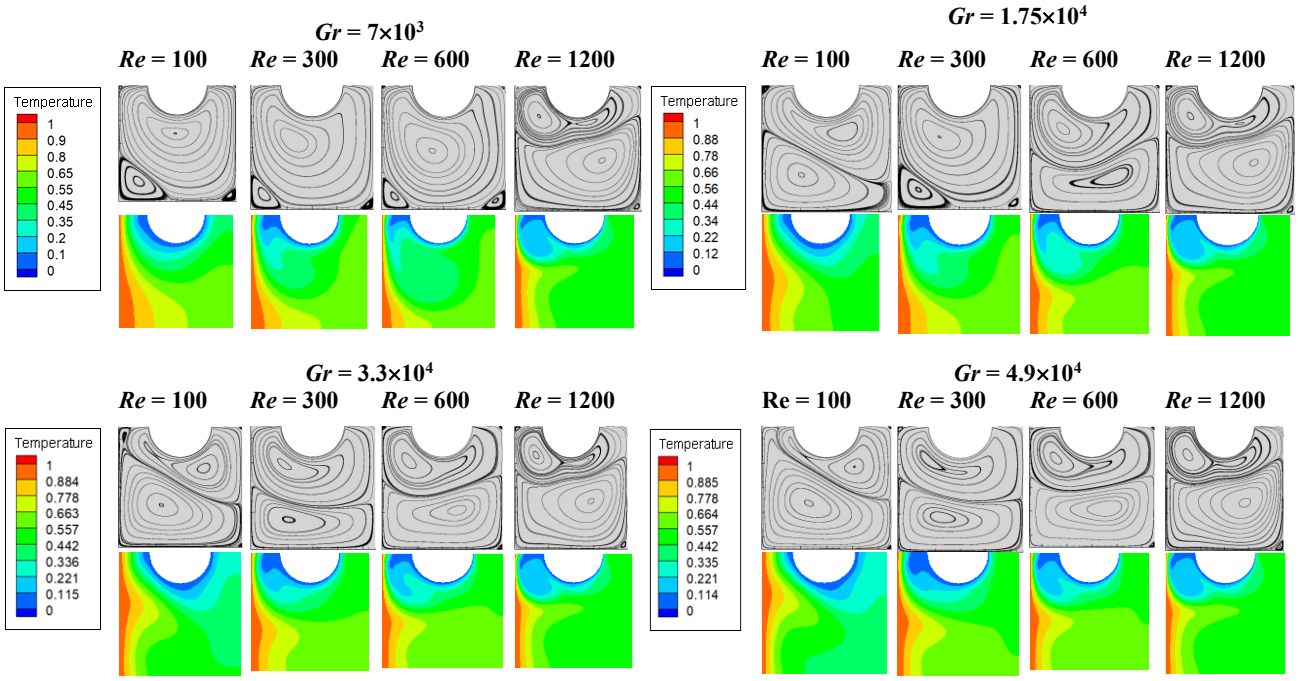

Fig 4 - Flow structure and thermal behavior for case A

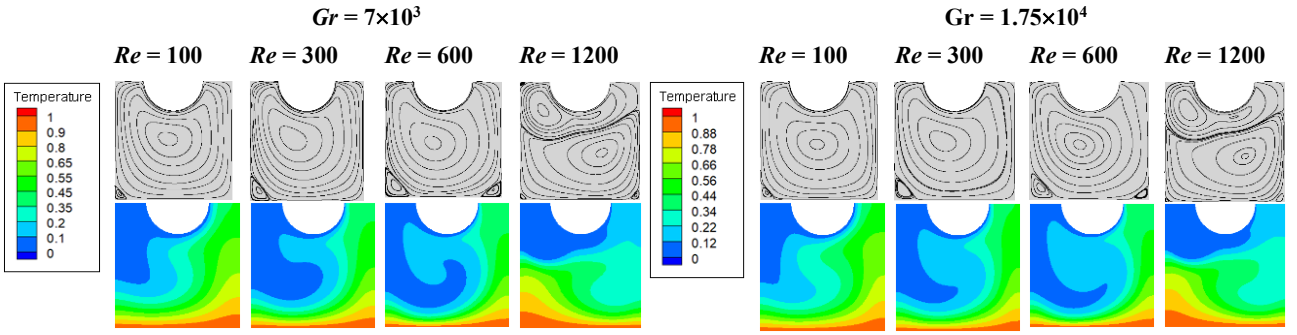

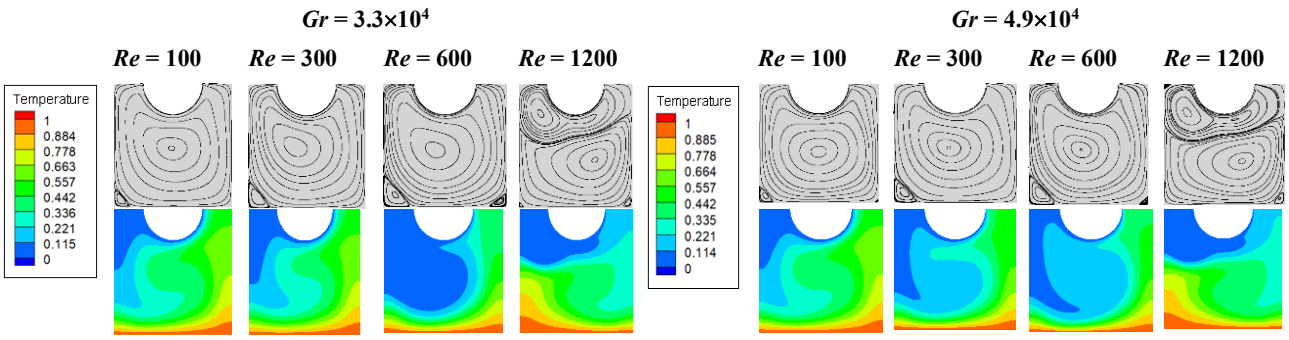

Fig 5 – Flow structure and thermal behavior for case B.

- **For case C.** Figure 6 shows the cavity with a hot left wall and a rotating cylinder on the right. Streamlines reveal two vertical vortices whose size depends on the dominant convection. At low *Gr*, forced convection prevails, making the right vortex larger. As *Gr* increases, natural convection becomes more influential, leading to the left-side vortex growing larger while the right-side vortex diminishes.

At moderate *Gr*, both vortices become similar in size, showing a transition between convection modes. For case C, higher *Re* enhances forced convection, transporting cold air more effectively to the cavity center and cooling that region. However, as *Gr* increases, natural convection dominates, raising overall air temperature and reducing cold zones.

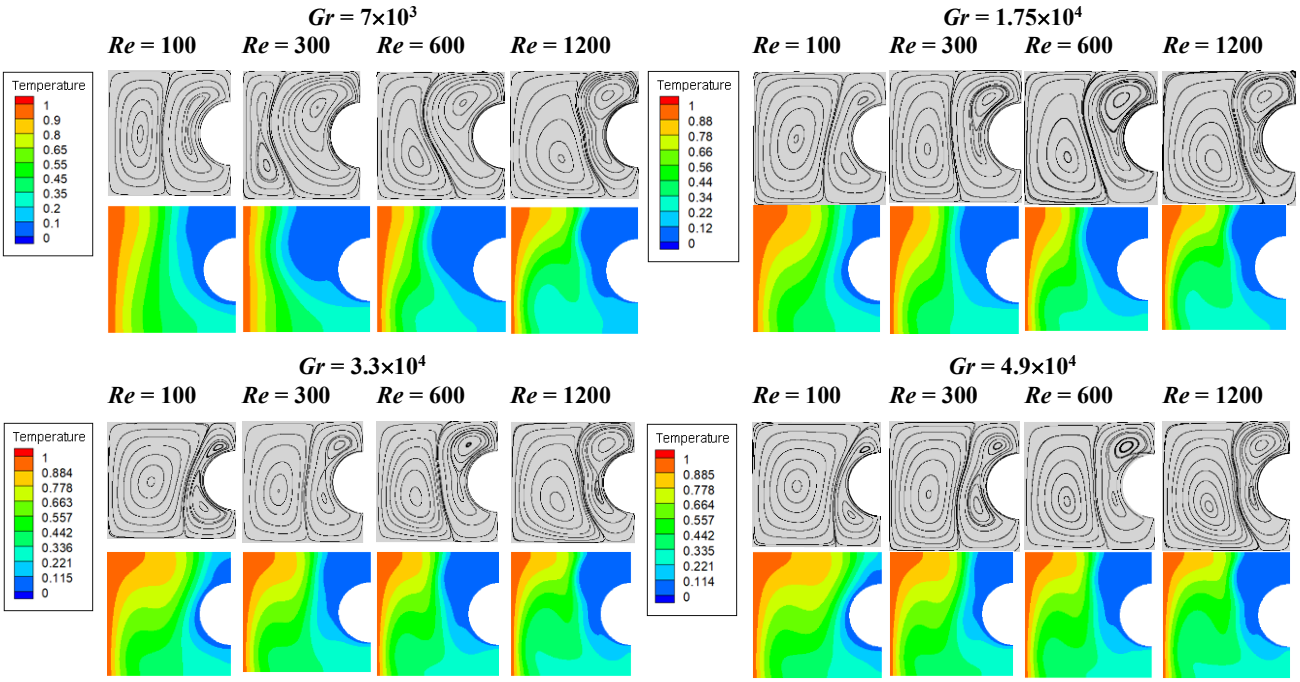

Fig 6 – Flow structure and thermal behavior for case C.

- **For case D.** Figure 7 shows the cavity with a hot left wall and a rotating cylinder at the bottom. Streamlines typically show two horizontal vortices, except at $Gr = 7\times10^3$ with $Re = 300$ and 600, where the top vortex is smaller and situated at the upper-left corner. At low *Gr* and *Re* from 100 to 600, forced convection dominates, resulting in a larger bottom vortex. As *Gr* increases, natural convection grows stronger, enlarging the top vortex. At $Re = 1\,200$, vortex sizes stabilize as the strong bottom-right vortex limits upward flow, reducing natural convection effects.

For case D, increasing *Re* enhances cold air transport to the cavity center. As *Gr* rises, cold regions shrink due to stronger natural convection and higher air temperatures. At $Re = 1200$, temperature distribution remains stable, and cold areas remain nearly unchanged.

5.2. Heat transfer rate analysis

Figure 8 presents the average Nusselt number (Nu) versus Richardson number (*Ri*) for the four cases (A, B, C, and D). In all cases, Nu decreases as *Ri* approaches 0.5 and then levels off for $Ri > 0.5$. Case A shows the highest Nu for $Ri \leq 0.5$, while case B has the highest for $Ri > 0.5$. Case D consistently outperforms case C. All cases exhibit fluctuations in Nu when $Ri < 0.2$. The maximum *Nu* ($Nu_{max} = 9.183$) is recorded in case A at $Ri = 0.034$ ($Re = 1200$, $Gr = 4.9\times10^4$), due to the small gap between the cold cylinder and the heated wall, which enhances the temperature gradient, and, consequently, enhanced heat transfer.

Figure 9 shows Nu increasing with *Re* in most cases. However, in case B, Nu increases initially but drops at $Re = 1\,200$. As *Gr* increases, *Nu* generally rises, except in case A, where it decreases and then stabilizes at higher *Gr* values, $Gr = 3.3\times10^4$ and 4.9×10^4.

In case D, at $Gr = 7\times10^3$, the average *Nu* is lower for $Re = 300$ and 600 due to a dominant single vortex and a smaller one in the top left. For other *Gr* and *Re* values, two vortices appear, with their size depending on whether forced or natural convection dominates. At low $Gr = 7000$ and $100 < Re < 600$, conduction dominates, and the rotating cylinder traps cold air on the adiabatic right side. When *Re* exceeds 600, convection takes over, improving cold air transport to the hot wall and increasing *Nu*.

Additionally, the effect of cylinder radius on heat transfer is examined for the best-performing case A at $Re = 1200$ and $Gr = 4.9\times10^4$. Figures 10 and 11 compare streamlines, temperature fields, and *Nu* for radii $R_0 = 0.2$, 0.5, and 0.8, offering better understanding into how cylinder size affects flow and heat transfer.

For a small cylinder radius ($R_0 = 0.2$), the top vortex is larger than the bottom. As the radius increases, the top vortex shifts to the upper-left corner and shrinks, while the bottom vortex grows. At $R_0 = 0.8$, the top vortex is smallest due to limited space. Figure 11 shows that a larger cylinder radius leads to a nearly linear increase in average *Nu*, due to stronger forced convection.

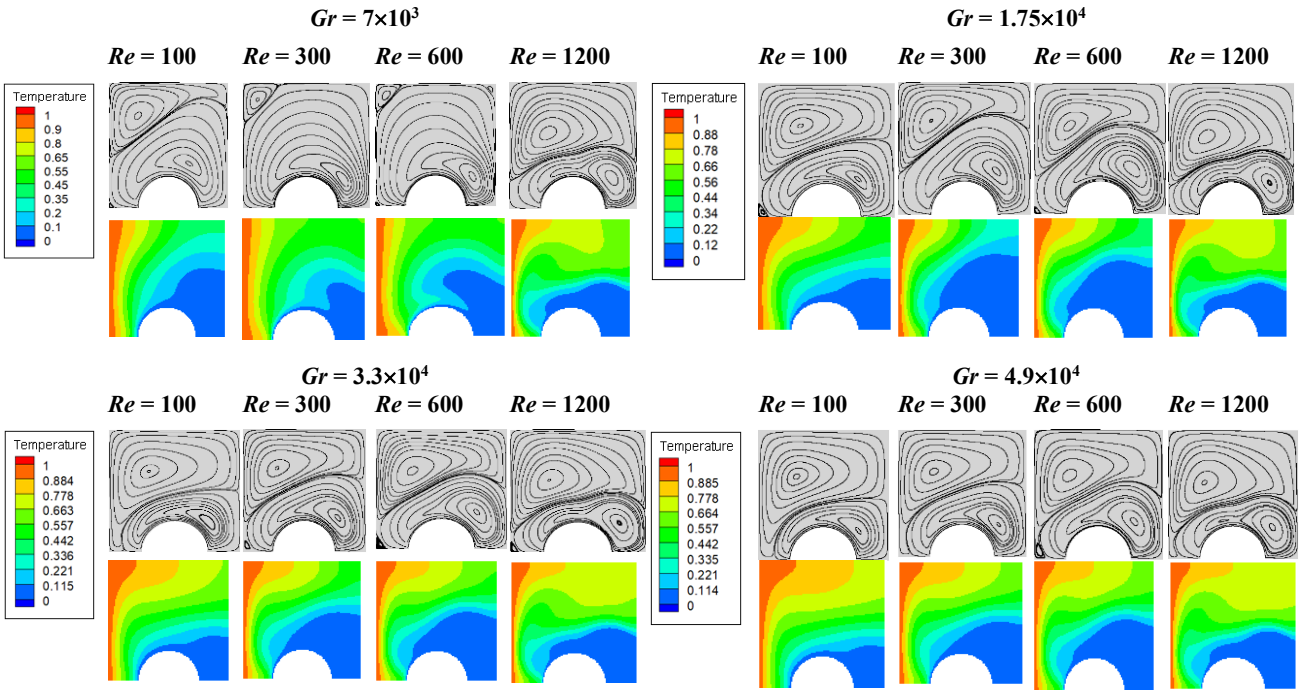

Fig 7 – Flow structure and thermal behavior for case D.

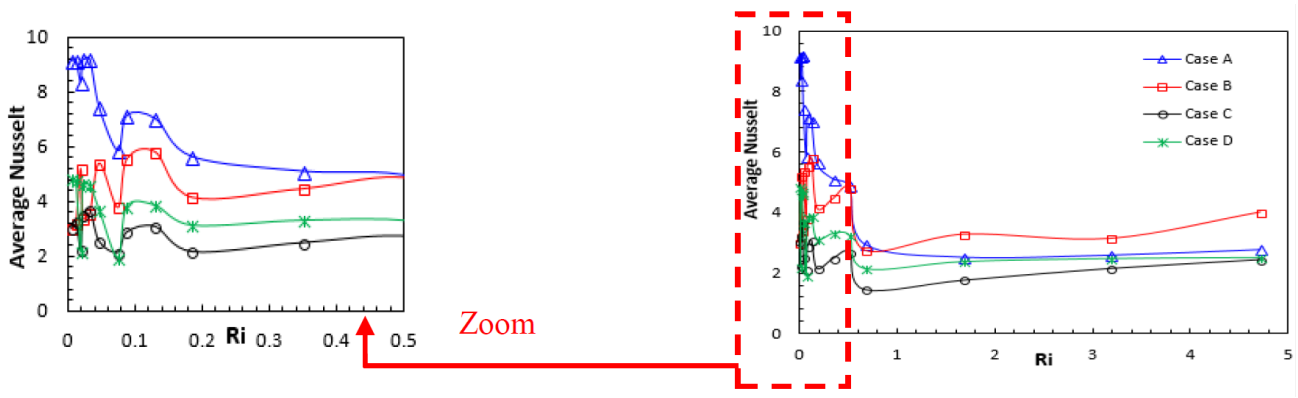

Fig 8 – Comparing the computed average Nusselt number against *Ri* number for each of the four cases under investigation (A, B, C, and D).

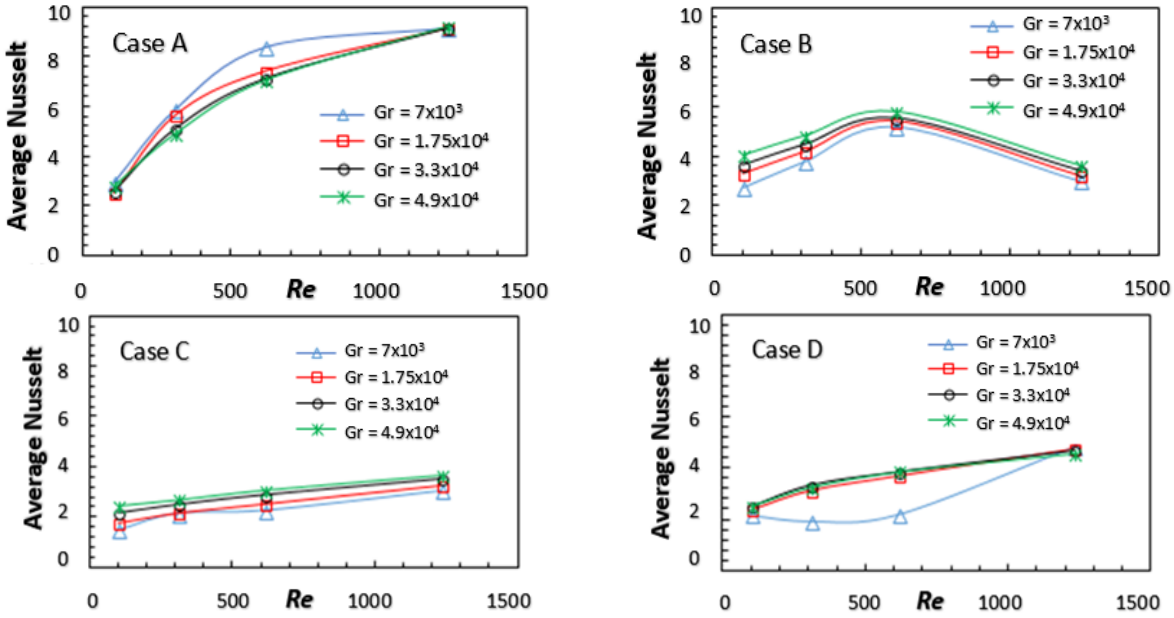

Fig 9 – Comparing the average Nusselt number versus Grashoft number *Gr* for cases under investigation (A, B, C, and D).

The study concludes that a rotating cylinder enhances heat transfer in a square cavity, with its position being critical. Case A (cylinder on the top wall, bottom wall heated) gives the highest *Nu*, while Case D (cylinder on the bottom wall, left wall heated) gives the lowest. Increasing cylinder size consistently boosts heat transfer. From an engineering perspective, the study emphasizes the value of numerical analysis for selecting optimal designs and developing new technologies.

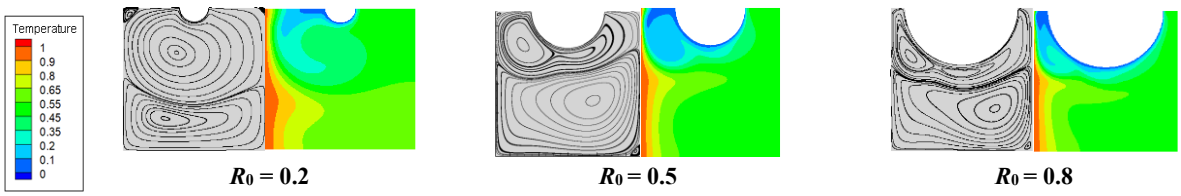

Fig. 10 – Effect of the rotating cylinder radius on the streamlines and temperature for the best performing case A at $Re = 1200$ and $Gr = 4.9 \times 10^4$.

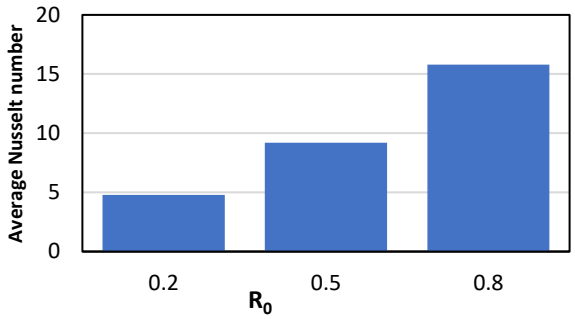

Fig 11 – Average Nusselt number versus the rotating cylinder radius for the best performing case A at $Re = 1200$ and $Gr = 4.9\text{x}10^4$.

6. CONCLUSION

This study conducted a comprehensive numerical investigation of laminar mixed convection in a square cavity with a rotating cylinder placed at various positions relative to different heated walls. Key thermal and flow parameters were varied, including Reynolds number ($100 \leq Re \leq 1200$), Grashof number ($7\times10^3 \leq \text{Gr} \leq 4.9\times10^4$), and cylinder radius ($R_0 = 0.2, 0.5, 0.8$), to identify configurations that optimize heat transfer. The main findings can be summarized as follows:

- Cylinder and heated wall positions significantly affect flow structure and heat transfer. Among all tested configurations, Case A (hot left wall + cylinder on the top wall) provided the best thermal performance, driven by strong interaction between cold fluid motion and the heated wall, especially at high *Re*.
- A distinct behavior of the average Nusselt number (*Nu*) with Richardson number (*Ri*) was observed: *Nu* decreases as *Ri* increases to 0.5, beyond which it stabilizes. Case A achieved a peak *Nu* of 9.183 at $Ri = 0.034$, corresponding to $Re = 1200$ and $Gr = 4.9\times10^4$. This represents a 250% improvement in heat transfer compared to Case C.
- Cylinder radius plays a key role in enhancing convective heat transfer. A nearly linear increase in Nu was observed with increasing R_0, due to the intensified flow velocity and more efficient disruption of thermal boundary layers. At $R_0 = 0.8$, flow recirculation becomes stronger, and thermal mixing is maximized.
- Flow patterns changes with *Re* and *Gr* values, revealing how the balance between natural and forced convection alters vortex structure. For example, in Case A, a dominant upper vortex interacts closely with the heated wall at high *Re* and provides higher thermal enhamcement, while in Case D, the lower-positioned cylinder and competing buoyancy forces result in weaker thermal enhancement.
- From an engineering design point, placing the rotating cylinder near the top wall with a heated sidewall maximizes thermal gradients and convective patterns, making this configuration ideal for compact thermal devices where enhanced heat removal is critical.

Finally, the study provides qualitative and quantitative evidence into how geometric arrangement, cylinder size, and flow parameters govern heat transfer in mixed convection systems. These findings help optimizing thermal management strategies in micro-devices, electronic cooling systems, and cavity-based heat exchangers.

REFERENCES

[1] Bejan A. Convection heat transfer. 3rd ed. New York: Wiley; 2004.
[2] Omari R. Numerical investigation of a mixed convection flow in a lid-driven cavity. American Journal of Computational Mathematics. 2016; 6: 251–258. DOI: 10.4236/ajcm.2016.63026
[3] Hussein AA. Mixed convection heat transfer in trapezoidal lid-driven cavity with uniformly heated inner circular cylinder. Archives of thermodynamics. 2023; 44: 99–118. DOI: 10.24425/ather.2023.147539
[4] Zhang Y, Lin H, Chaturvedi R, Singh PK, Mansir IB, Zhang K, Alhoee J. Mixed convection of EG/NEPCM inside a lid driven cavity with a rotating cylinder. Case Studies in Thermal Engineering. 2023, 47: 103072. DOI: 10.1016/j.csite.2023.103072
[5] Oztop HF, Zhao Z, Yu B, Fluid flow due to combined convection in lid-driven enclosure having a circular body. Int. J. Heat Fluid Flow. 2009; 30: 886–901. DOI: 10.1016/j.ijheatfluidflow.2009.04.009
[6] Muneer AI. Numerical solution of mixed convection in a lid-driven cavity with arc-shaped moving wall. Engineering Computations. 2017; 34: 869–891. DOI: 10.1108/EC-11-2015-0368

[7] Kandasamy R, Wang X, Mujumdar AS. Transient cooling of electronics using phase change material (PCM)-based heat sinks. Appl. Therm. Eng. 2008; 28: 1047–1057. DOI: 10.1016/j.applthermaleng.2007.06.010
[8] Alvarez A, Cabeza O, Muñiz MC, Varela LM. Experimental and numerical investigation of a flat-plate solar collector. Energy. 2010; 35: 3707–3716. Doi: 10.1016/j.energy.2010.05.016
[9] Wang SM, Shen ZG, Gu LX. Numerical simulation of buoyancy-driven turbulent ventilation in attic space under winter conditions. Energy Build. 2012; 47: 360–368. DOI: 10.1016/j.enbuild.2011.12.012
[10] Öztop HF, Sakhrieh A, Abu-Nada E, Al-Salem K. Mixed convection of MHD flow in nanofluid filled and partially heated wavy walled lid-driven enclosure. International Communications in Heat and Mass Transfer. 2017; 86: 42–51. DOI: 10.1016/j.icheatmasstransfer.2017.05.011
[11] Ali Khaleel K, Gao S. Mixed convection heat transfer enhancement in a cubic lid-driven cavity containing a rotating cylinder through the introduction of artificial roughness on the heated wall. Physics of Fluids. 2018; 30: 025103. DOI: 10.1063/1.5017474
[12] Lavasani AM, Farhadi M, Rabienataj Darzi AA. Study of convection heat transfer enhancement inside lid driven cavity utilizing fins and nanofluid. Thermal science. 2017; 21(6A): 2431–2442. DOI: 10.2298/TSCI150125158L
[13] Selimefendigil F, Öztop HF, Mixed convection of ferrofluids in a lid driven cavity with two rotating cylinders. Engineering Science and Technology, an International Journal. 2015; 18: 439–451. DOI: 10.1016/j.jestch.2015.03.003
[14] Munshi MJH, Alim MA, Bhuiyan AH, Ali M. Hydrodynamic mixed convection in a lid- driven square cavity including elliptic shape heated block with corner heater. Procedia Engineering. 2017; 94, 442–449. DOI: 10.1016/j.proeng.2017.08.169
[15] Gangawane KM, Manikandan B. Mixed convection characteristics in lid-driven cavity containing heated triangular block. Chinese Journal of Chemical Engineering. 2017; 25: 1381–1394. DOI: 10.1016/j.cjche.2017.03.009
[16] Biswas N, Manna NK, Mahapatra PS. Enhanced thermal energy transport using adiabatic block inside lid-driven cavity. Int. J. Heat Mass Transfer. 2016; 100: 407–427. DOI: 10.1016/j.ijheatmasstransfer.2016.04.074
[17] Islam AW, Sharif MAR, Carlson ES. Laminar mixed convection in a lid driven square cavity with two isothermally heated square internal blockages. Chemical. Engineering. Communications. 2015; 202, 1176–1190. DOI: 10.1080/00986445.2014.912634
[18] Filali A, Khezzar L, Semmari H, Matar O. Application of Artificial Neural Network for mixed convection in square lid-driven cavity with double vertical or horizontal oriented rectangular blocks. International Communications in Heat and Mass Transfer. 2021; 129: 105644. DOI: 10.1016/j.icheatmasstransfer.2021.105644
[19] Vieira RS, Petry AP, Rocha LAO, Isoldi LA, Dos Santos ED. Numerical evaluation of a solar chimney geometry for different ground temperatures by means of Constructal design. Renew. Energy. 2017; 109: 222–234. DOI: 10.1016/j.renene.2017.03.007
[20] Barros GM, Lorenzini G, Isoldi LA, Rocha LAO, Dos Santos ED. Influence of mixed convection laminar flows on the geometrical evaluation of a triangular arrangement of circular cylinders. Int. J. Heat Mass Transf. 2017; 114: 1188–1200. DOI: 10.1016/j.ijheatmasstransfer.2017.07.010
[21] Dos Santos ED, Isoldi LA, Souza JA, Goulart MM, Rodrigues MK, Seibt FM, De Souza RV, Rocha LAO, Constructal design of a rectangular fin intruded into forced convective lid-driven cavity flows. In: Proc. Constr. Law Conf. 1. 2013, p. 126–134. DOI: 10.1115/1.4033378
[22] Lorenzini G, Machado BS, Isoldi LA, Dos Santos ED, Rocha LAO. Constructal design of rectangular fin intruded into mixed convective lid-driven cavity flows. ASME-J. Heat Transf. 2016; 138: 102501. DOI: 10.1115/1.4033378
[23] Hussain SH, Hussein AK. Mixed convection heat transfer in a differentially heated square enclosure with a conductive rotating circular cylinder at different vertical locations. Int. Commun. Heat Mass Transf. 2011; 38: 263–274. DOI: 10.1016/j.icheatmasstransfer.2010.12.006
[24] Park YG, Yoon HS, Ha MY. Natural convection in square enclosure with hot and cold cylinders at different vertical locations, Int. J. Heat Mass Transf. 2012; 5: 7911–7925. DOI: 10.1016/j.ijheatmasstransfer.2012.08.012
[25] Razera AL, Fagundes TM, Seibt FM, Da Fonseca RJC, Varela DJ, Ortiz PRB, Coelho FR, Lessa LZ, Schmidt A, Furtado GM, Dos Santos ED, Isoldi LA, Rocha LAO, Constructal design of a triangular fin inserted in a cavity with mixed convection lid-driven flow. Defect Diffus. Forum. 2016; 372: 188–201. DOI: 10.4028/www.scientific.net/DDF.372.188
[26] Razera AL, Da Fonseca RJC, Isoldi LA, Dos Santos ED, Rocha LAO, Biserni C. Constructal design of a semi-elliptical fin inserted in a lid-driven square cavity with mixed convection. International Journal of Heat and Mass Transfer. 2018; 126: 81–94. DOI: 10.1016/j.ijheatmasstransfer.2018.05.157
[27] Patankar SV. Numerical heat transfer and fluid flow. Taylor and Francis; 1980.
[28] Krane RJ, Jessee J. Some detailed field measurements for a natural convection flow in a vertical square enclosure. In: 1st ASME-JSME Thermal Engineering Joint Conference. 1983.

Received December 21, 2024